

## Muscone Protects Vertebral End-plate Degeneration by Antiinflammatory Property

Qian-Qian Liang PhD, Min Zhang PhD,  
Quan Zhou MD, PhD, Qi Shi MD, Yong-Jun Wang MD, PhD

Received: 27 July 2008 / Accepted: 25 August 2009 / Published online: 18 September 2009  
© The Association of Bone and Joint Surgeons® 2009

**Abstract** Most chronic neck pain is the result of degeneration of the cervical spine. IL-1 $\beta$  may play an important role in intervertebral disc degeneration. This being the case, inhibiting IL-1 $\beta$  could provide a therapeutic approach for reducing or preventing disc degeneration. Muscone reportedly relieves pain and suppresses inflammation. Therefore, we asked whether muscone, a potent antiinflammatory agent, could reduce proinflammatory cytokines in vitro (end-plate

cartilage cultures) and end-plate degeneration in vivo (a rat model that induces intervertebral disc degeneration). In vitro, muscone reversed IL-1 $\beta$ -induced upregulation of IL-1 $\beta$ , tumor necrosis factor  $\alpha$ , cyclooxygenase 2, inducible nitric oxide synthase, matrix metalloproteinase 13, aggrecanase 2, and nitric oxide and downregulation of Col2 $\alpha$ 1 and aggrecan. Pretreatment with muscone (6.25, 12.5, 25  $\mu$ mol/L) inhibited the IL-1 $\beta$ -induced phosphorylation of extracellular signal-regulated kinases 1/2 and c-Jun N-terminal kinase in a dose-dependent manner. In vivo, muscone inhibited the expression of prostaglandin E2, 6-keto-prostaglandin F1 $\alpha$ , IL-1 $\beta$ , and tumor necrosis factor  $\alpha$  and recovered the structural distortion of the degenerative disc. Our findings suggest muscone is a promising agent for treating intervertebral disc degeneration through its antiinflammatory effects.

One or more of the authors (YJW, MZ) received funding from the National Science Fund for Distinguished Young Scholars (30625043), the International Cooperation Programs of National Natural Science Foundation of China (30710103904), the Key Project of National Natural Science Foundation of China (30330700), the International Technical Cooperation Key Project Plan, Chinese Science and Technology Committee Emphasis (2006DFA32670), the Project of National Natural Science Foundation of China (30701118, 30600829, and 30572398), and Science and Technology Commission of Shanghai “outstanding academic leaders” program (08XD1404000). Each author certifies that his or her institution has approved the animal protocol for this investigation and that all investigations were conducted in conformity with ethical principles of research. This work was performed at the Institute of Spine, Shanghai University of Traditional Chinese Medicine.

Q.-Q. Liang, M. Zhang, Q. Zhou, Q. Shi, Y.-J. Wang (✉)  
Institute of Spine, 725 Wan-Ping South Road, Shanghai 200032,  
China  
e-mail: yjwang88@hotmail.com

Q.-Q. Liang, M. Zhang, Q. Zhou, Q. Shi, Y.-J. Wang  
Department of Orthopaedics & Traumatology, Longhua  
Hospital, Shanghai University of Traditional Chinese Medicine,  
Shanghai, China

Q. Zhou  
Department of Orthopaedic Surgery, University of Rochester  
Medical Center, Rochester, NY, USA

### Introduction

Neck pain is one of the most common chronic conditions affecting the quality of life and sometimes causing disability in adults. Most chronic neck pain is the result of degeneration of intervertebral discs (IVDs) in the cervical spine [2, 3]. An intact end-plate cartilage is critical for normal IVD functions, as the major nutrient supply of IVDs is diffused through end plates [18, 45]. Pathologic changes in end-plate cartilage are closely related to IVD degeneration [45] and thus to cervical spondylopathy. Prevention and reduction of lesions in the vertebral end plate therefore are high research priorities.

Although the etiopathogenesis of IVD degeneration is not completely understood, it is believed sustained production of the proinflammatory cytokine IL-1 $\beta$  in the affected IVD may play a pivotal role in degeneration [23].

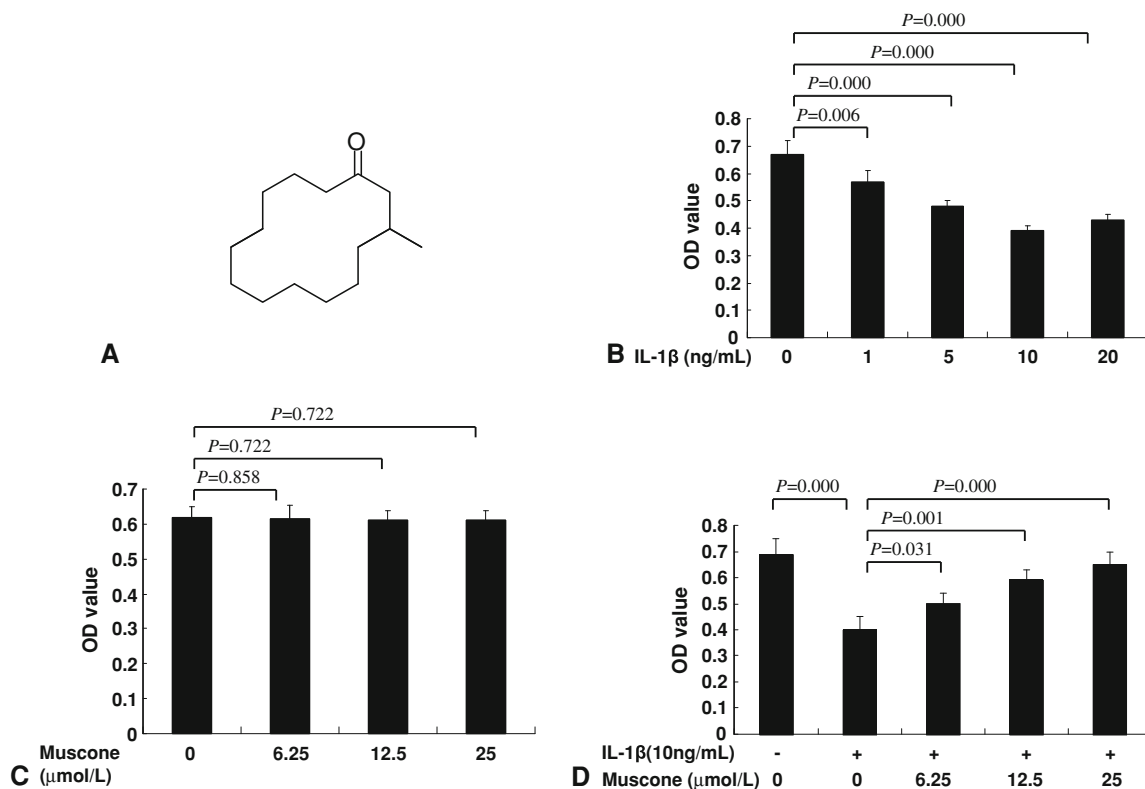


**Fig. 1A–D** (A) A diagram shows the chemical structure of muscone (3-methylcyclopentadecanone). (B) IL-1 $\beta$  (0–20 ng/mL) inhibits the viability of end-plate chondrocytes in a dose-dependent manner. (C) Muscone alone does not have any effect on the viability of end-plate

chondrocytes. (D) Muscone blocked the IL-1 $\beta$ -induced cytotoxic effects in a dose-dependent manner. Values are shown as means (bars) + SDs (error bars) of three independent experiments. OD = optical density.

Although IL-1 $\beta$  is synthesized by the normal end-plate chondrocytes in physiologic conditions, its overproduction disturbs the normal balance of catabolic and anabolic events with an increase in degradative enzymes and a decrease in the expression of genes for matrix proteins [15, 23, 24]. Also, IL-1 $\beta$  transcriptionally induces the expression of cyclooxygenase 2 (COX-2) [39] associated with sciatica and radiculopathy [40, 46] and stimulates the production of prostaglandin E2 (PGE2), which also may cause pain [28, 36]. IL-1 also stimulates nitric oxide (NO) production and inducible nitric oxide synthase (iNOS) expression in disc cells [17, 21], and NO serves as a key signaling molecule, participating in the induction of apoptosis and modulation of proteoglycan and collagen production in disc cells [11, 14, 34]. IL-1 $\beta$  triggers several signaling cascades in chondrocytes, including activation of extracellular signal-regulated kinases p42/p44 (ERK1/2), c-Jun N-terminal kinase (JNK), and mitogen-activated protein kinase P38 (P38-MAPK) [20, 35]. As a result, expression of COX-2 and iNOS promotes inflammation, and upregulation of matrix metalloproteinases (MMPs) may induce degradation of Type II collagen [9, 10, 27, 31, 33]. Thus, blocking IL-1 $\beta$ 's effect on end-plate cartilage

may help in identifying novel therapeutic targets for IVD degeneration [6, 16].

Musk, an odoriferous animal product, has been widely used in China for treatment of sprains and fractures. It is believed musk improves local microcirculation and relieves pain caused by chronic inflammation [26, 30, 42]. Until the late 19th century, musk was obtained only from natural sources. However, in current traditional Chinese medicine, natural musk has been replaced mostly with its chemically synthesized counterparts. These compounds can be divided into three major classes: aromatic nitro musks, polycyclic musk compounds, and macrocyclic musk compounds. Muscone (3-methylcyclopentadecanone) (Fig. 1A), one of the macrocyclic musk compounds, primarily is responsible for the characteristic odor of musk and is able to relieve pain and suppress inflammation [26, 41]. In China, some traditional Chinese medicine doctors use muscone to effectively treat neck pain [38].

We therefore asked whether muscone could (1) block the effect of a proinflammatory factor (IL-1 $\beta$ ) on end-plate chondrocytes in vitro, (2) inhibit inflammatory cytokine expression in degenerated IVD, and (3) prevent IVD degeneration in vivo.

## Materials and Methods

In vitro, we isolated chondrocytes from the end-plate cartilage of the cervical spine of rats. Chondrocytes were incubated in serum-free medium overnight and then different concentrations of IL-1 $\beta$  with or without muscone in 0.5% fetal bovine serum (FBS) were added. Chondrocytes cultured with no IL-1 $\beta$  or muscone served as controls. In replicate (three) experiments, we determined cell proliferation and NO production and examined mRNA expression of IL-1 $\beta$ , tumor necrosis factor  $\alpha$  (TNF- $\alpha$ ), COX-2, iNOS, MMP-13, aggrecanase 2 (ADAMTS-5), Col2 $\alpha$ 1, and aggrecan by real-time PCR analysis. Subconfluent end-plate chondrocytes in monolayer cultures were switched to serum-free medium for 12 hours, treated with muscone for 6 hours, and then treated with IL-1 $\beta$  for 30 minutes. Cell lysates were prepared and Western blot was performed for phosphorylation of JNK, ERK1/2, and P38-MAPK. The Chinese local Animal Ethics Committee approved collection of the IVD samples and chondrocytes.

In vivo, we randomly assigned 30 rats, 3 months old, for control (n = 10), surgery (n = 10), and muscone (n = 10) groups. Rats in the surgery and muscone groups underwent surgery (excision of the paraspinal muscles and the supraspinous and interspinous ligaments from C2–C7) that results in IVD degeneration [47]. Four months later, rats in the muscone group were fed muscone once a day for 30 days. Five months after surgery or sham surgery, the cervical spines of all rats were harvested for hematoxylin and eosin staining, in situ hybridization, and ELISA analysis. The ELISA results were repeated three times. All experiments were performed under the auspices of the Animal Ethics Committee.

In replicate (three) experiments, we isolated primary chondrocytes from the end-plate cartilage of the cervical spine of three 4-week-old Sprague-Dawley rats. The cartilage end plate of six C3–C7 intervertebral spaces were removed carefully from the vertebrate and minced into small pieces (< 0.3 mm<sup>3</sup>). Twelve samples were digested sequentially with 0.2% trypsin (Sigma-Aldrich, St Louis, MO) at 37°C for 20 minutes followed by 0.02% collagenase (Sigma) at 37°C for 24 hours. The digested tissue was filtered through a 100- $\mu$ m cell strainer (BD Biosciences, Bedford, MA). Cells were washed with phosphate-buffered saline and then plated at a density of  $2 \times 10^4$  cells/cm<sup>2</sup> in tissue culture flasks and cultured in Dulbecco's Modified Eagle Medium (DMEM; Gibco, New York, NY) supplemented with 10% FBS (HyClone, Logan, UT) and 1% penicillin/streptomycin (Invitrogen, Carlsbad, CA) in a humidified 5% CO<sub>2</sub> at 37°C. Cells cultured at Passage 1 were used for the experiments. Cells were counted with a hemacytometer and cultured at  $1 \times 10^5$  cells per well in 2 mL growth medium in six-well plates (Corning, New York, NY).

We placed  $1 \times 10^4$  cells each in two 96-well plates and cultured them in 0.1 mL DMEM supplemented with 10% FBS. After culture for 1 day, such cells were incubated in serum-free medium overnight and then every six wells were treated with IL-1 $\beta$  (0, 1, 5, 10, and 20 ng/mL), muscone (0, 6.25, 12.5, and 25  $\mu$ mol/L) (Biomol, Plymouth Meeting, PA), or IL-1 $\beta$  (10 ng/mL) with muscone (6.25, 12.5, and 25  $\mu$ mol/L) in 0.5% FBS for 24 hours. The viability of end-plate chondrocytes was determined using a MTT (3-[4, 5-dimethylthiazol-2-yl]-2, 5-diphenyl tetrazolium bromide)-based cell proliferation and viability assay kit according to the instructions of the manufacturer (R&D Systems, Minneapolis, MN).

We placed  $1 \times 10^5$  cells each in five wells of a six-well plate (Corning) and cultured them in 2 mL DMEM supplemented with 10% FBS. After culture for 3 days, such cells were incubated in serum-free medium overnight and then treated with IL-1 $\beta$  (0 and 10 ng/mL) or IL-1 $\beta$  (10 ng/mL) + muscone (6.25, 12.5, and 25  $\mu$ mol/L) in 0.5% FBS for 24 hours. RNA was harvested using an RNeasy® kit (Qiagen, Valencia, CA) according to the manufacturer's protocol. Total RNA (1  $\mu$ g) was reverse-transcribed using the Advantage™ RT-for-PCR kit (Qiagen) following the manufacturer's protocol. Freshly reverse-transcribed cDNA was used for real-time PCR using SYBR® Green (Bio-Rad, Hercules, CA) to monitor DNA synthesis. The primers for Col2 $\alpha$ 1, aggrecan, IL-1 $\beta$ , TNF- $\alpha$ , COX-2, iNOS, MMP-13, ADAMTS-5, and  $\beta$ -actin were designed by TaKaRa Biotechnology Co Ltd (Otsu, Shiga, Japan), and the target sites on genes and PCR product length are shown in Table 1. PCR was performed using the Rotor-Gene™ real-time DNA amplification system (Corbett Research, Sydney, Australia) using the following cycling protocol: a 95°C denaturation step for 5 minutes followed by 40 cycles of 95°C denaturation (20 seconds), 62°C annealing (20 seconds), and 72°C extension (20 seconds). Detection of the fluorescent product was performed at the end of the 72°C extension period. Gene expression was normalized to  $\beta$ -actin. PCR products were subjected to melting curve analysis, and the data were analyzed and quantified using Rotor-Gene™ 6.0 analysis software analysis software (Corbett Research).

We placed  $1 \times 10^5$  cells each in two six-well plates and cultured them in 2 mL DMEM supplemented with 10% FBS. After culture for 3 days, the two six-well plates were switched to serum-free medium for 12 hours. Chondrocytes of four wells of one plate were treated with IL-1 $\beta$  (0, 1, 5, and 10 ng/mL), and chondrocytes of four wells of the other plate were treated with IL-1 $\beta$  (0 ng/mL) + muscone (0  $\mu$ mol/L) or IL-1 $\beta$  (10 ng/mL) + muscone (6.25, 12.5, and 25  $\mu$ mol/L); both plates' chondrocytes were cultured for 24 hours. We determined nitrite levels of the culture medium through indirect measurement of the NO production using the Greiss method as described by Evans et al. [7]. We

**Table 1.** Summary of primer designs synthesized according to published rat sequences

Factor	Sense/antisense	Primer sequence (5' → 3')	Product size (bp)
Col2 $\alpha$ 1	Sense	TCCTAAGGGTGCCAATGGTGA	112
	Antisense	AGGACCAACTTTGCCTTGAGGAC	
MMP-13	Sense	CCCTGGAGCCCTGATGTTT	142
	Antisense	CTCTGGTGTTTTGGGGTGCT	
IL-1 $\beta$	Sense	AGGTCGTCATCATCCCACGAG	120
	Antisense	GCTGTGGCAGCTACCTATGTCTTG	
COX-2	Sense	GGAGCATCCTGAGTGGGATGA	145
	Antisense	AAGCAGGTCTGGGTGCGAACTTG	
TNF- $\alpha$	Sense	CCACGCTCTTCTGTCTACTG	145
	Antisense	GCTACGGGCTTGTCACCTC	
iNOS2	Sense	CTCACTGTGGCTGTGGTCACCTA	101
	Antisense	GGGTCTTCGGGCTTCAGGTTA	
Aggrecan	Sense	CCAGATCATCACTACGCAGTCCTC	101
	Antisense	TCCGCTGGTCTGATGGACAC	
ADAMTS-5	Sense	TCAGGGATCCTCACAACGTCAG	135
	Antisense	GCATCATCGGCTCAAAGCTACA	
$\beta$ -actin	Sense	GGAGATTACTGCCCTGGCTCCTA	150
	Antisense	GACTCATCGTACTCCTGCTTGCTG	

MMP-13 = matrix metalloproteinase 13; IL-1 $\beta$  = interleukin 1 $\beta$ ; COX-2 = cyclooxygenase 2; TNF- $\alpha$  = tumor necrosis factor  $\alpha$ ; iNOS2 = inducible nitric oxide synthase 2; ADAMTS-5 = aggrecanase 2.

placed  $1 \times 10^5$  cells each in five wells of a six-well plate and cultured them in 2 mL DMEM supplemented with 10% FBS. After culture for 3 days, the six-well plates were switched to serum-free medium for 12 hours. Chondrocytes of four wells were treated with muscone (0, 6.25, 12.5 and 25  $\mu\text{mol/L}$ ) for 6 hours and then treated with IL-1 $\beta$  (10 ng/mL) for 30 minutes; another well without any treatment served as a control. The end-plate chondrocytes were lysed in Golden lysis buffer supplemented with protease inhibitor (Boehringer Mannheim, Indianapolis, IN), 1 mmol/L sodium orthovanadate, 1 mmol/L ethyleneglycol-bis-( $\beta$ -aminoethyl ether), 1 mmol/L sodium fluoride, and 1  $\mu\text{mol/L}$  microcysteine (Sigma). Protein concentrations were quantified using the Coomassie Plus<sup>TM</sup> Protein Assay Kit (Bio-Rad). Thirty micrograms of protein was separated by SDS-PAGE and then transferred to a PVDF membrane (NEN Life Science Products Inc, Boston, MA). The blots were probed overnight at 4°C with rabbit anti-rat phosphor-JNK antibody (Cell Signaling Technology Inc, Danvers, MA), phosphor-ERK 1/2 antibody (Upstate Biotechnology Inc, Lake Placid, NY), or phosphor-P38 antibody (Upstate Inc). After washing, the membranes were incubated for 1 hour at 20°C with goat anti-rabbit-immunoglobulin G (Oncogene, Boston, MA). Immune complexes were detected using Odyssey<sup>®</sup> Infrared Imaging System (LI-COR Bioscience Inc, Lincoln, NE). Membranes were reprobated for  $\beta$ -actin to confirm equal protein loading. We repeated the experiment three times.

Thirty 3-month-old Sprague-Dawley rats were obtained from the Shanghai Laboratory Animal Center of the Chinese Academy of Science and were randomly assigned to one of three groups (control, surgery, or muscone), with five male and five female rats in each group. Rats in the control group underwent sham surgery. The skin in the nuchal area was incised but immediately closed thereafter. Rats in the surgery group were anesthetized and their paraspinal muscles from C2–C7 were exposed and excised from a midline nuchal incision over the posterior cervical spine [47]. In addition, the supraspinous and interspinous ligaments were sharply excised at each level. The third experimental group was designated the muscone group. Four months after the real surgery, rats were fed 10 mg muscone per kg once a day for 30 days. Five months after the real or sham surgery, all rats were euthanized using 100 mg pentobarbitone sodium per kg (Nembutal<sup>®</sup>; Boehringer Ingelheim, North Ryde, Australia), and their cervical spines were harvested for analysis.

We collected eight en bloc specimens of the IVDs with the adjacent vertebral end plates from the C4–C5 level. They were fixed, decalcified, dehydrated, clarified with dimethylbenzene, and embedded in olefin. At least four consecutive 7- $\mu\text{m}$  sections were prepared at the median-sagittal planes and stained using hematoxylin and eosin and toluidine blue. The morphologic features of the cartilage end plate, annulus fibrosus, and nucleus pulposus were observed using an Olympus BX 50 microscope (Olympus,

Tokyo, Japan), and TNF- $\alpha$ -labeled cell numbers were determined using a semiautomated image autoanalysis system (CMIAS-99B, Okolab, Milan, Italy). The histologic evaluations were performed by an independent pathologist (CJZ) who specializes in musculoskeletal histology/pathology and was blind to the intervention.

The TNF- $\alpha$  probe was purchased from Boehringer Mannheim. Radiolabeled probes were produced by transcribing linearized antisense cDNA in the presence of [<sup>33</sup>P]UTP (Amersham, Little Chalfont, UK) using T3 or T7 polymerases at 37°C for 2 hours. Template DNA was degraded using RNase-free DNase (Qiagen). The labeled RNA was purified through a MicroSpin™ G-50 column (Amersham, Pharmacia Biotech, Piscataway, NJ), and radioactivity counts were determined. Sense probes were used as negative controls. After dewaxing and rehydration, sagittal sections of end-plate cartilage were pretreated with a standard hybridization buffer. Hybridization was performed at 55°C for 24 hours. Nonspecific binding was hydrolyzed by adding 20  $\mu$ g/mL RNase A. The slides subsequently were incubated in 5x sodium chloride-sodium citrate buffer/40 mmol/L  $\beta$ -mercaptoethanol and 50% formamide/1x sodium chloride-sodium citrate buffer/40 mmol/L  $\beta$ -mercaptoethanol at 55°C. Kodak NTB-2 emulsion-dipped slides were exposed for 5 to 14 days and autoradiography was performed using Kodak film (Eastman Kodak Co, Rochester, NY). TNF- $\alpha$ -labeled cells were counted using the semiautomated image autoanalysis system (CMIAS-99B).

We homogenized eight C5–C6 IVD and cartilage end-plate tissue samples of equal mass by ultrasonication in an ice bath. The homogenates were centrifuged at 13,000 rpm for 3 minutes at room temperature. PGE2, IL-1 $\beta$ , and 6-keto-prostaglandin F1 $\alpha$  (6-K-PGF1 $\alpha$ ) in the supernatant were measured using commercial ELISA kits (R&D Systems).

Data are expressed as means with SDs. We assessed whether our data met the assumption for normal distribution by performing the Kolmogorov-Smirnov test. Our data met the assumption for normal distribution (mRNA expression of IL-1 $\beta$ :  $p = 0.269$ ; mRNA expression of COX-2:  $p = 0.148$ ; mRNA expression of TNF- $\alpha$ :  $p = 0.142$ ; mRNA expression of Col2 $\alpha$ 1:  $p = 0.783$ ; mRNA expression of aggrecan:  $p = 0.973$ ; mRNA expression of MMP-13:  $p = 0.343$ ; mRNA expression of ADAMTS-5:  $p = 0.906$ ; mRNA expression of iNOS:  $p = 0.988$ ; cell viability treated by IL-1 $\beta$ :  $p = 0.924$ ; cell viability treated by muscone:  $p = 0.905$ ; cell viability treated by IL-1 $\beta$  and muscone:  $p = 0.997$ ; NO production treated by IL-1 $\beta$ :  $p = 0.942$ ; NO production treated by IL-1 $\beta$  and muscone:  $p = 0.840$ ; ELISA test of PGE2:  $p = 0.781$ ; ELISA test of 6-K-PGF1 $\alpha$ :  $p = 0.990$ ; ELISA test of IL-1 $\beta$ :  $p = 0.972$ ; and TNF- $\alpha$ -labeled cell numbers:  $p = 0.972$ ). The following were compared using ANOVA and post hoc testing

using Dunnett's *t* test: differences in cell viability among different IL-1 $\beta$  doses (0, 1, 5, 10, and 20 ng/mL) and different muscone doses (0, 6.25, 12.5, and 25  $\mu$ mol/L); differences in NO production among different IL-1 $\beta$  doses (0, 1, 5, 10, and 20 ng/mL); differences in cell viability, NO production, and relative gene expression levels among 10 ng/mL IL-1 $\beta$  and four other different treatments (0 ng/mL IL-1 $\beta$  + 0  $\mu$ mol/L muscone, 10 ng/mL IL-1 $\beta$  + 6.25  $\mu$ mol/L muscone, 10 ng/mL IL-1 $\beta$  + 12.5  $\mu$ mol/L muscone, 10 ng/mL IL-1 $\beta$  + 25  $\mu$ mol/L muscone) *in vitro*; and differences in TNF- $\alpha$ -labeled cell numbers and protein contents of PGE2, 6-K-PGF1 $\alpha$ , and IL-1 $\beta$  among control, surgery, and muscone groups. Statistical analysis was performed using SPSS® 10.0 (SPSS Inc, Chicago, IL).

## Results

Muscone blocked the effect of IL-1 $\beta$  on the end-plate chondrocytes *in vitro*. Treatment with IL-1 $\beta$  reduced the viability of the end-plate chondrocytes in a dose-dependent manner (Fig. 1B). The addition of muscone alone did not negatively affect the viability of end-plate chondrocytes (Fig. 1C) but blocked the IL-1 $\beta$ -induced cytotoxic effects *in vitro* (Fig. 1D). In end-plate chondrocytes, exogenous IL-1 $\beta$  resulted in an increase of endogenous IL-1 $\beta$ , TNF- $\alpha$ , and COX-2 mRNA expression, but treatment with 25  $\mu$ mol/L muscone reduced the three cytokines induced by exogenous IL-1 $\beta$  (Fig. 2). In end-plate chondrocytes, nitrite levels were induced by IL-1 $\beta$ . The response was attenuated by muscone in a dose-dependent manner, especially by 25  $\mu$ mol/L muscone. Furthermore, stimulation with IL-1 $\beta$  (10 ng/mL) upregulated the mRNA level of iNOS, which also was blocked by 25  $\mu$ mol/L muscone (Fig. 3). In addition, IL-1 $\beta$  (10 ng/mL) downregulated Col2 $\alpha$ 1 and aggrecan, whereas it upregulated MMP-13 and ADAMTS-5. However, 25  $\mu$ mol/L muscone increased mRNA expression of Col2 $\alpha$ 1 and aggrecan and downregulated MMP-13 and ADAMTS-5 induced by IL-1 $\beta$  (Fig. 4). In addition, the phosphorylation levels of ERK1/2, JNK, and P38-MAPK were increased by stimulation of IL-1 $\beta$  (10 ng/mL) for 30 minutes. Pretreatment with muscone (6.25–25  $\mu$ mol/L) inhibited phosphorylation levels of ERK1/2 and JNK in a dose-dependent manner. However, pretreatment with as much as 25  $\mu$ mol/L muscone did not suppress phosphorylation of P38-MAPK (Fig. 5).

Muscone showed antiinflammatory action *in vivo*. The concentration of PGE2, 6-K-PGF1 $\alpha$ , and IL-1 $\beta$  were greater in the IVD homogenates of the surgery group than in the control group, but the muscone group showed lower concentrations than the surgery group (Fig. 6). *In situ* hybridization showed the number of TNF- $\alpha$ -labeled cells in the cartilage end plate was higher in the surgery group than

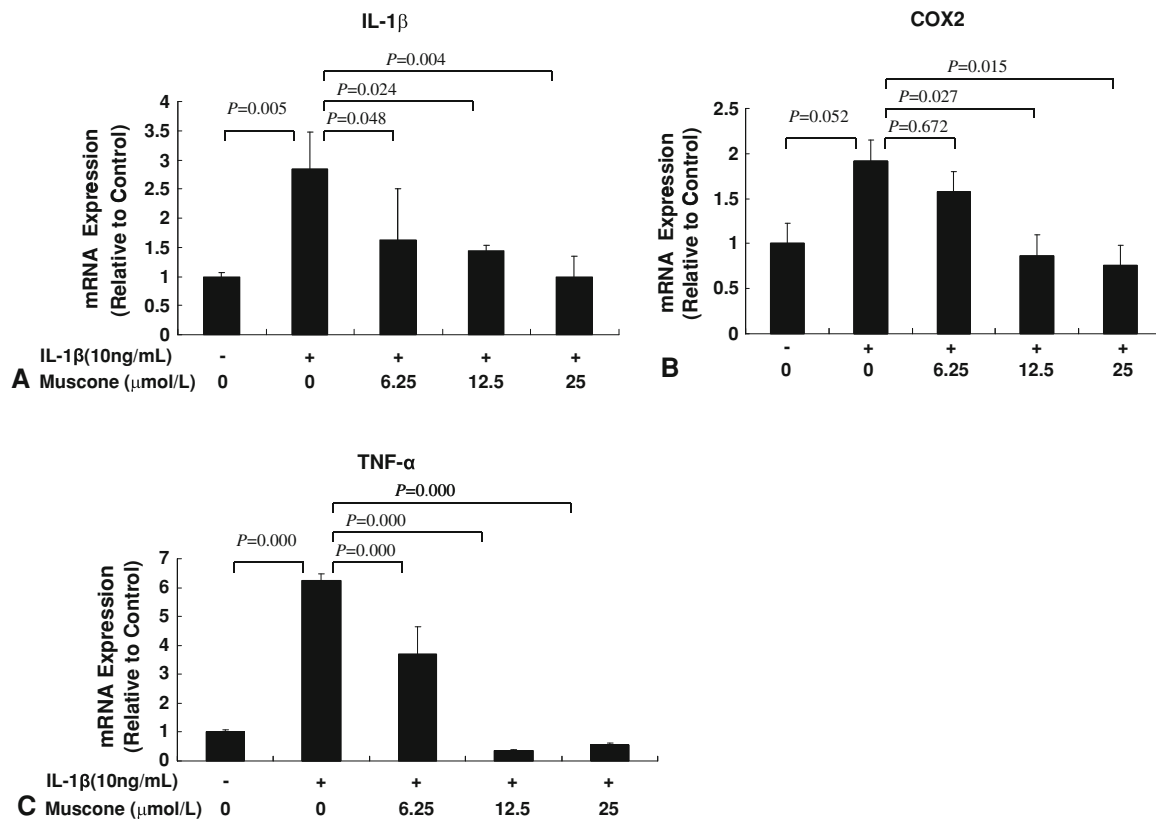


**Fig. 2A–C** Muscone inhibited mRNA expression of (A) IL-1 $\beta$ , (B) COX-2, and (C) TNF- $\alpha$  in a dose-dependent manner. Values are shown as means (bars) + SDs (error bars) of three independent experiments.

in the control group but was reduced in the muscone group compared with the surgery group (Fig. 7A–B).

Muscone inhibited disc degeneration. The mice receiving muscone (10 mg/kg) treatment for 30 days had no obvious adverse reactions or side effects. Histologic examination of the C4–C5 IVDs and adjacent end-plate cartilage of the control group samples showed a normal, well-organized annulus fibrosus surrounding an intact nucleus pulposus. The cartilage end plate was organized to superficial non-calcified and deeper calcified cartilage layers. In the surgery group samples, the fibers of the annulus fibrosus were disoriented and fragmented. The nucleus pulposus was shrunken and disorganized. Muscone treatment almost completely restored the structural characteristics of the spine subjected to accelerated degeneration from surgery. The morphologic features of the IVDs and end-plate cartilage were close to normal in the muscone group (Fig. 7C).

## Discussion

Degenerated discs spontaneously generate increased amounts of inflammatory mediators, especially IL-1 $\beta$ , which not only stimulates the release of degenerative

enzymes such as MMPs but also inhibits synthesis of extracellular matrix proteins [32, 37]. Inhibition of IL-1 $\beta$  can be an important therapeutic approach for preventing and reversing disc degeneration [6]. Muscone relieves pain and suppresses inflammation [26, 41]. We therefore hypothesized muscone could block the effect of a proinflammatory factor (IL-1 $\beta$ ) on end-plate chondrocytes in vitro, inhibit inflammatory cytokine expression, and prevent IVD degeneration in degenerated IVDs in vivo.

Several limitations to this study should be noted. First, in our in vitro study, we did not examine the effect of muscone on the protein level of inflammatory mediators. Obviously not all changes in gene expression are translated into protein expression and our findings require confirmation at the protein level. Second, we studied select inflammatory regulators and cannot make conclusions about others. Third, in our in vivo study, we used only one IVD degeneration animal model; different kinds of animal models should be used in additional studies to confirm our conclusions. Showing muscone retards end-plate cartilage degeneration by its antiinflammatory effects does not necessarily mean it will protect the annulus fibrosus and nucleus pulposus. Additional in vitro study of cells isolated from the annulus fibrosus and nucleus pulposus is needed.

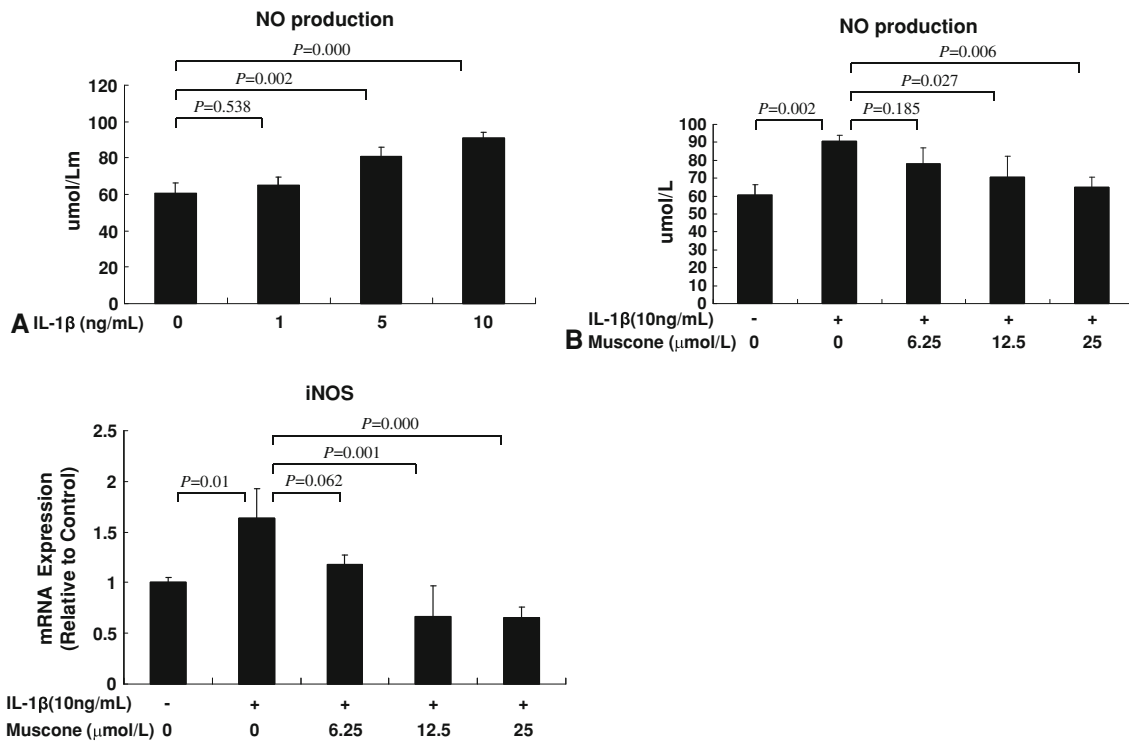


**Fig. 3A–C** (A) IL-1 $\beta$  (0–10 ng/mL) induced NO production of end-plate chondrocytes in a dose-dependent manner. (B) Muscine suppressed IL-1 $\beta$ -induced NO production in a dose-dependent

manner. (C) Muscine downregulated IL-1 $\beta$ -induced iNOS mRNA expression in a dose-dependent manner. Values are shown as means (bars) + SDs (error bars) of three independent experiments.

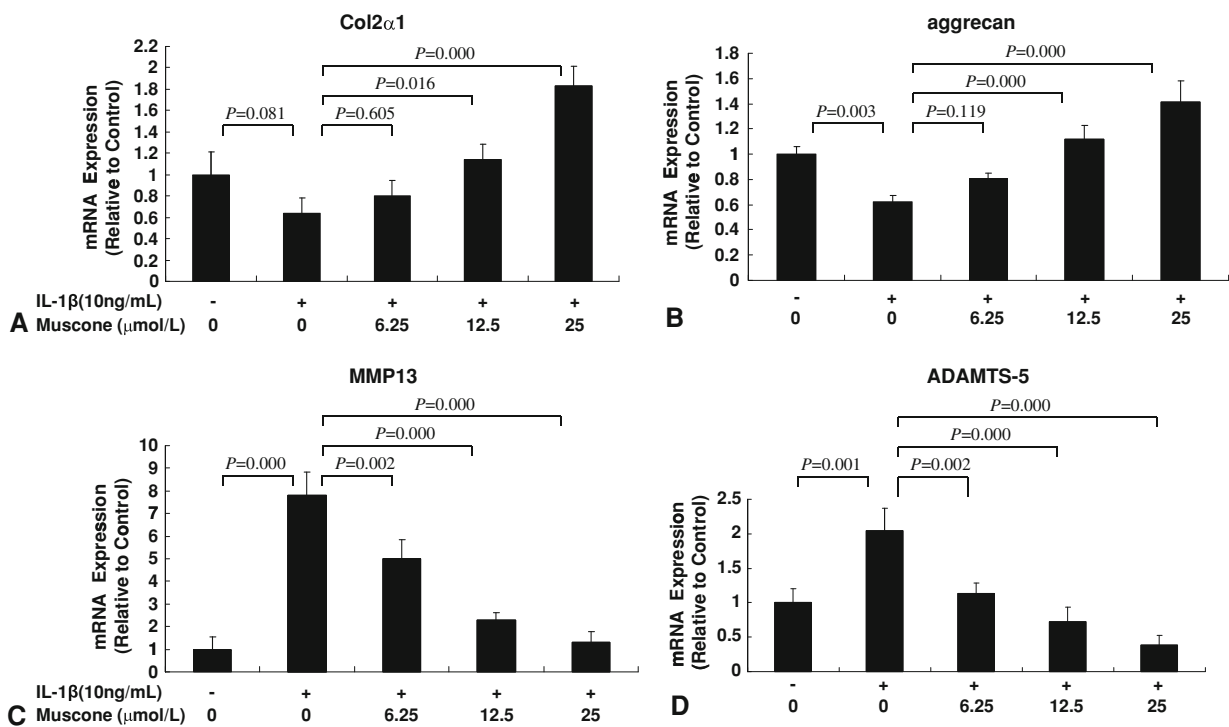


**Fig. 4A–D** Muscine inhibited IL-1 $\beta$ -induced downregulation of (A) Col2 $\alpha$ 1 and (B) aggrecan mRNA expression and IL-1 $\beta$ -induced upregulation of (C) MMP-13 and (D) ADAMTS-5 mRNA expression.

Values are shown as means (bars) + SDs (error bars) of three independent experiments.

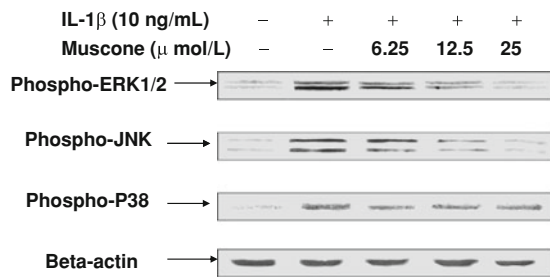


**Fig. 5** The phosphorylation levels of ERK 1/2, JNK, and P38-MAPK were increased by stimulation of IL-1 $\beta$  (10 ng/mL) for 30 minutes. Pretreatment with muscone (6.25–25  $\mu$ mol/L) inhibited IL-1 $\beta$ -induced phosphorylation of ERK 1/2 and JNK in a dose-dependent manner. However, pretreatment with as much as 25  $\mu$ mol/L muscone did not suppress phosphorylation of P38-MAPK.

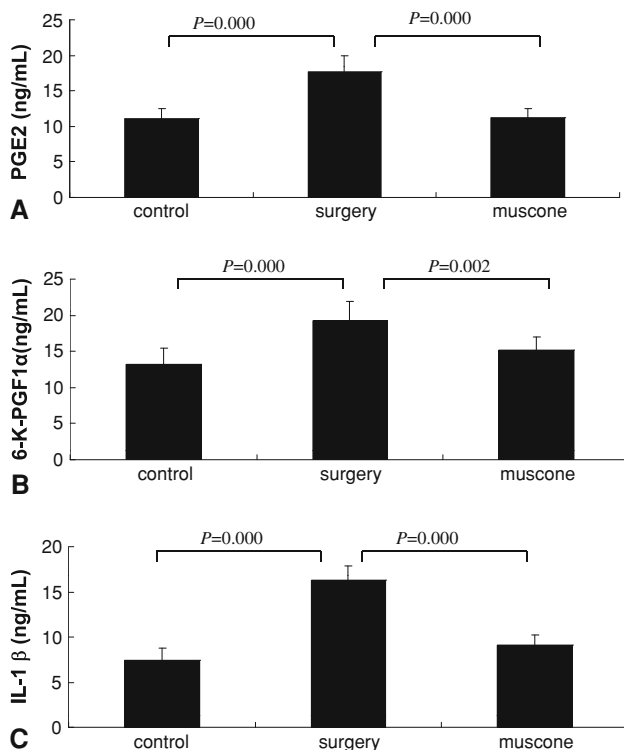


**Fig. 6A–C** Muscone inhibited the concentration of (A) PGE2, (B) 6-K-PGF1 $\alpha$ , and (C) IL-1 $\beta$  in tissue homogenates of the IVDs ( $n = 8$  samples per treatment group). Values are shown as means (bars) + SDs (error bars) of three independent experiments.

We investigated whether muscone could block the effect of IL-1 $\beta$  on end-plate chondrocytes *in vitro* because IL-1 $\beta$  stimulates the release of degenerative enzymes such as MMPs [25] and inhibits synthesis of extracellular matrix proteins [10]; IL-1 $\beta$  will stimulate and IL-1 receptor antagonist will inhibit matrix degradation in intact human IVD tissue [15]. Previous reports suggested IL-1 $\beta$  is a key cytokine mediating matrix degradation in the IVD and therefore is a therapeutic target [6, 10, 15, 16, 23–25]. Our data suggest, in end-plate chondrocytes, cell viability and

expression of aggrecan and Type II collagen genes were downregulated, whereas matrix-degrading proteases (MMP-13 and ADAMTS-5), and the investigated cytokines and NO production, were induced by IL-1 $\beta$ . These findings are consistent with those of previous studies [5, 8, 19, 43]. In our study, muscone inhibited those activities of IL-1 $\beta$  and suggested muscone is an anti-IL-1 $\beta$  agent.

We then examined the effect of muscone on the downstream signal factors of IL-1 $\beta$  and found muscone blocked activation of JNK and ERK1/2 but not P38-MAPK. Although there are no reports suggesting whether inhibition of ERK1/2 and JNK could provide a therapeutic approach to slow the course of IVD degeneration, some studies of articular chondrocytes have indicated inhibition of ERK1/2 and JNK downregulates MMPs and effectively treats rheumatoid arthritis [22, 44]. In addition to regulation of MMPs, ERK also modulates Type II collagen expression [13] and regulates COX-2 expression and PGE2 production [48]. Those studies suggest the inhibitory effects of muscone on generation of IL-1 $\beta$  and the pro-catabolic function of IL-1 $\beta$  arise from inhibition of the JNK and ERK1/2 signal pathways. Additional studies are needed to determine the mechanisms responsible for inhibition of muscone on ERK1/2 and JNK in end-plate chondrocytes.

After identifying the effect of muscone on end-plate chondrocytes *in vitro*, we determined whether muscone could inhibit the expression of inflammatory factors and prevent IVD degeneration *in vivo*. We examined the effect of muscone on an IVD degeneration animal model. Our data suggest the cervical disc of the surgery group had severe degenerative changes with the increase of inflammatory cytokines (TNF- $\alpha$ , IL-1 $\beta$ , PGE2, and 6-K-PGF1 $\alpha$ ), consistent with results of previous reports that degenerated discs spontaneously generate increased amounts of inflammatory mediators [24, 47]. However, in our study, muscone reduced expression of those inflammatory mediators and almost completely restored the structural characteristics of the spine subjected to accelerated degeneration from surgery.

Our *in vivo* and *in vitro* studies suggested muscone prevented IVD degeneration by its antiinflammatory effect. It has been reported muscone prevents and treats complications of myocardial infarct [49]. Naturally occurring muscone from the group of macrocyclic musk compounds, a group of substances that have not yet been well characterized with respect to their toxicologic properties, is active *in vitro* with a hormonelike effect [1]. It has been reported synthetic musk fragrance compounds have agonistic activities toward human estrogen receptors  $\alpha$  and  $\beta$  and have antagonistic activity toward the human androgen receptor [29]. Also, the effect of hormonelike substances on cartilage cells has been described [12]. The hormonelike



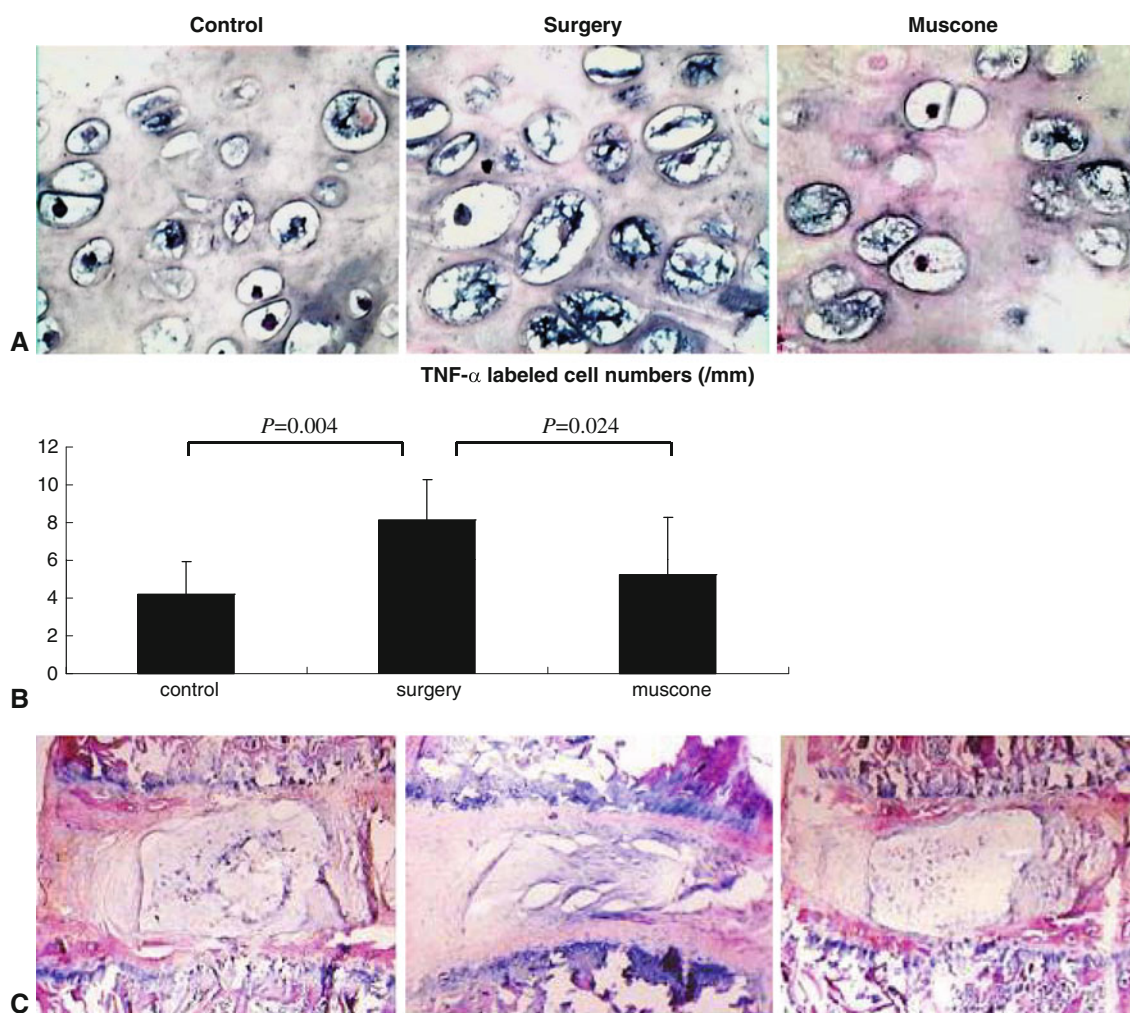


**Fig. 7A–C** (A) The number of TNF- $\alpha$ -positive cells was increased in the surgery group compared with controls but was close to normal in the muscone group (Stain, in situ hybridization staining; original magnification,  $\times 400$ ). (B) Mean values are shown for the number of TNF- $\alpha$ -positive cells in three groups (values shown as means

[bars] + SDs [error bars]). (C) In the surgery group, the laminar structures of the annulus fibrosus were disorganized, and the nucleus pulposus was fibrotic and fissured. Muscone treatment almost completely reversed the IVD degeneration caused by surgery (Stain, hematoxylin and eosin; original magnification,  $\times 100$ ).

effect of muscone might explain its antiinflammatory effect on IVD. Muscone also can enter the brain through the blood-brain barrier [4], which might be the mechanism underlying the muscone attraction to the end plate. A complete pharmacodynamic study examining the systemic transportation and local distribution of muscone is the focus of a future investigation.

Our data suggest muscone may block the effect of a proinflammatory factor (IL-1 $\beta$ ) on the end-plate chondrocytes in vitro, inhibit inflammatory cytokine expression in degenerated IVDs, and prevent IVD degeneration in vivo. We believe muscone is a promising drug for therapy of diseases related to IVD degeneration.

**Acknowledgments** We thank Drs. Lawrence G. Raisz, University of Connecticut Health Center, Farmington, CT, Yrjo T. Kontinen, University of Helsinki, Helsinki, Finland, and Tian-Fang Li,

University of Connecticut Health Center, for constructive discussion in relation to the experimental design and language revision. We also thank Dr. Chong Jian Zhou, Institute of Spine, Shanghai University of Traditional Chinese Medicine, for the histologic evaluations.

## References

- Bitsch N, Dudas C, Körner W, Failing K, Biselli S, Rimkus G, Brunn H. Estrogenic activity of musk fragrances detected by the E-screen assay using human mcf-7 cells. *Arch Environ Contam Toxicol.* 2002;43:257–264.
- Borghouts JA, Koes BW, Bouter LM. The clinical course and prognostic factors of non-specific neck pain: a systematic review. *Pain.* 1998;77:1–13.
- Centeno CJ, Fleishman J. Degenerative disc disease and pre-existing spinal pain. *Ann Rheum Dis.* 2003;62:371–372.
- Chen WK, Huang YF, Wang HD. An experimental study on distribution of musk into the brain through blood brain barrier. *Zhong Xi Yi Jie He Xue Bao.* 2004;2:288–291.

5. de Isla NG, Mainard D, Muller S, Stoltz JF. In vitro effects of diacerein on NO production by chondrocytes in response to proinflammatory mediators. *Biomed Mater Eng*. 2008;18(1 suppl): S99–S104.
6. Evans C. Potential biologic therapies for the intervertebral disc. *J Bone Joint Surg Am*. 2006;88:95–98.
7. Evans CH, Watkins SC, Stefanovic-Racic M. Nitric oxide in cartilage metabolism. *Methods Enzymol*. 1996;269:75–88.
8. Fan Z, Bau B, Yang H, Soeder S, Aigner T. Freshly isolated osteoarthritic chondrocytes are catabolically more active than normal chondrocytes, but less responsive to catabolic stimulation with interleukin-1beta. *Arthritis Rheum*. 2005;52:136–143.
9. Fan Z, Söder S, Oehler S, Fundel K, Aigner T. Activation of interleukin-1 signaling cascades in normal and osteoarthritic articular cartilage. *Am J Pathol*. 2007;171:938–946.
10. Fan Z, Yang H, Bau B, Söder S, Aigner T. Role of mitogen-activated protein kinases and NFkappaB on IL-1beta-induced effects on collagen type II, MMP-1 and 13 mRNA expression in normal articular human chondrocytes. *Rheumatol Int*. 2006;26: 900–903.
11. Furusawa N, Baba H, Miyoshi N, Maezawa Y, Uchida K, Kokubo Y, Fukuda M. Herniation of cervical intervertebral disc: immunohistochemical examination and measurement of nitric oxide production. *Spine*. 2001;26:1110–1116.
12. Gaissmaier C, Koh JL, Weise K. Growth and differentiation factors for cartilage healing and repair. *Injury*. 2008;39(suppl 1):S88–S96.
13. Gilbert SJ, Blain EJ, Duance VC, Mason DJ. Sphingomyelinase decreases type II collagen expression in bovine articular cartilage chondrocytes via the ERK signaling pathway. *Arthritis Rheum*. 2008;58:209–220.
14. Goldring MB, Birkhead J, Sandell LJ, Kimura T, Krane SM. Interleukin-1 suppresses expression of cartilage-specific type II and IX collagens and increases type I and III collagens in human chondrocytes. *J Clin Invest*. 1988;82:2026–2031.
15. Hoyland JA, Le Maitre C, Freemont AJ. Investigation of the role of IL-1 and TNF in matrix degradation in the intervertebral disc. *Rheumatology (Oxford)*. 2008;47:809–814.
16. Jimbo K, Park JS, Yokosuka K, Sato K, Nagata K. Positive feedback loop of interleukin-1beta upregulating production of inflammatory mediators in human intervertebral disc cells in vitro. *J Neurosurg Spine*. 2005;2:589–595.
17. Kang JD, Goergescu HI, McIntyre-Larkin L, Stefanovic-Racic M, Donaldson W, Evans CH. Herniated lumbar intervertebral discs spontaneously produce matrix metalloproteinases, nitric oxide, interleukin-6, and prostaglandin E2. *Spine*. 1996;21:271–277.
18. Katz MM, Hargens AR, Garfin SR. Intervertebral disc nutrition: diffusion versus convection. *Clin Orthop Relat Res*. 1986;210: 243–245.
19. Kim KS, Cho HS, Lee SD, Kim KH, Cho JY, Chung KH, Lee YC, Moon SK, Kim CH. Inhibitory effect of *Buthus martensi* Karsch extracts on interleukin-1beta-induced expression of nitric oxide (NO) synthase and production of NO in human chondrocytes and LPS-induced NO and prostaglandin E2 production in mouse peritoneal macrophages. *Toxicol In Vitro*. 2005;19: 757–769.
20. Kim YJ, Hwang SY, Oh ES, Oh S, Han IO. IL-1beta, an immediate early protein secreted by activated microglia, induces iNOS/NO in C6 astrocytoma cells through p38 MAPK and NF-kappaB pathways. *J Neurosci Res*. 2006;84:1037–1046.
21. Kohyama K, Saura R, Doita M, Mizuno K. Intervertebral disc cell apoptosis by nitric oxide: biological understanding of intervertebral disc degeneration. *Kobe J Med Sci*. 2000;46:283–295.
22. Legendre F, Bogdanowicz P, Martin G, Domagala F, Leclercq S, Pujol JP, Ficheux H. Rhein, a diacerein-derived metabolite, modulates the expression of matrix degrading enzymes and the cell proliferation of articular chondrocytes by inhibiting ERK and JNK-AP-1 dependent pathways. *Clin Exp Rheumatol*. 2007;25: 546–555.
23. Le Maitre CL, Freemont AJ, Hoyland JA. The role of interleukin-1 in the pathogenesis of human intervertebral disc degeneration. *Arthritis Res Ther*. 2005;7:R732–R745.
24. Le Maitre CL, Hoyland JA, Freemont AJ. Catabolic cytokine expression in degenerate and herniated human intervertebral discs: IL-1beta and TNF-alpha expression profile. *Arthritis Res Ther*. 2007;9:R77.
25. Le Maitre CL, Pockert A, Buttle DJ, Freemont AJ, Hoyland JA. Matrix synthesis and degradation in human intervertebral disc degeneration. *Biochem Soc Trans*. 2007;35:652–655.
26. Lin DL, Chang HC, Huang SH. Characterization of allegedly musk-containing medicinal products in Taiwan. *J Forensic Sci*. 2004;49:1187–1193.
27. Mendes AF, Caramona MM, Carvalho AP, Lopes MC. Role of mitogen-activated protein kinases and tyrosine kinases on IL-1-Induced NF-kappaB activation and iNOS expression in bovine articular chondrocytes. *Nitric Oxide*. 2002;6:35–44.
28. Miyamoto H, Saura R, Harada T, Doita M, Mizuno K. The role of cyclooxygenase-2 and inflammatory cytokines in pain induction of herniated. *Kobe J Med Sci*. 2000;46:13–28.
29. Mori T, Iida M, Ishibashi H, Kohra S, Takao Y, Takemasa T, Arizono K. Hormonal activity of polycyclic musks evaluated by reporter gene assay. *Environ Sci*. 2007;14:195–202.
30. Morishita S, Mishima Y, Shoji M. Pharmacological properties of musk. *Gen Pharmacol*. 1987;18:253–261.
31. Ogata S, Kubota Y, Yamashiro T, Takeuchi H, Ninomiya T, Suyama Y, Shirasuna K. Signaling pathways regulating IL-1alpha-induced COX-2 expression. *J Dent Res*. 2007;86:186–191.
32. Podichetty VK. The aging spine: the role of inflammatory mediators in intervertebral disc degeneration. *Cell Mol Biol*. 2007;53:4–18.
33. Radons J, Bosserhoff AK, Grassel S, Falk W, Schubert TE. p38MAPK mediates IL-1-induced down-regulation of aggrecan gene expression in human chondrocytes. *Int J Mol Med*. 2006;17: 661–668.
34. Rannou F, Rchette P, Benallaoua M, François M, Genries V, Korwin-Zmijowska C, Revel M, Corvol M, Poiraudou S. Cyclic tensile stretch modulates proteoglycan production by intervertebral disc annulus fibrosus cells through production of nitrite oxide. *J Cell Biochem*. 2003;90:148–157.
35. Scherle PA, Pratta MA, Feeser WS, Tancula EJ, Arner EC. The effects of IL-1 on mitogen-activated protein kinases in rabbit articular chondrocytes. *Biochem Biophys Res Commun*. 1997; 230:573–577.
36. Schweizer A, Feige U, Fontana A, Müller K, Dinarello CA. Interleukin-1 enhances pain reflexes: mediation through increased prostaglandin E2 levels. *Agents Actions*. 1988;25:246–251.
37. Sobajima S, Shimer AL, Chadder RC, Kompel JF, Kim JS, Gilbertson LG, Kang JD. Quantitative analysis of gene expression in a rabbit model of intervertebral disc degeneration by real-time polymerase chain reaction. *Spine J*. 2005;5:14–23.
38. Sun P. Analysis of medical records of cervical spondylopathy. *Shanghai J Traditional Chinese Med*. 2004;38:27–28.
39. Swiergiel AH, Dunn AJ. Distinct roles for cyclooxygenases 1 and 2 in interleukin-1-induced behavioral changes. *J Pharmacol Exp Ther*. 2002;302:1031–1036.
40. Taiwo YO, Levine JD. Effects of cyclooxygenase products of arachidonic acid metabolism on cutaneous nociceptive threshold in the rat. *Brain Res*. 1990;537:372–374.
41. Takabe K, Sugiura M, Asumi Y, Mase N, Yoda H, Shimizu H. Practical optical resolution of dl-muscone using tartaric acid derivatives as a chiral auxiliary. *Tetrahedron Lett*. 2005;46: 3457–3460.

42. Taneja V, Siddiqui HH, Arora RB. Studies on the anti-inflammatory activity of *Moschus moschiferus* (musk) and its possible mode of action. *Indian J Physiol Pharmacol.* 1973;17:241–247.
43. Toegel S, Wu SQ, Piana C, Unger FM, Wirth M, Goldring MB, Gabor F, Viernstein H. Comparison between chondroprotective effects of glucosamine, curcumin, and diacerein in IL-1beta-stimulated C-28/I2 chondrocytes. *Osteoarthritis Cartilage.* 2008; 16:1205–1212.
44. Tsutsumi R, Ito H, Hiramitsu T, Nishitani K, Akiyoshi M, Kitaori T, Yasuda T, Nakamura T. Celecoxib inhibits production of MMP and NO via down-regulation of NF-kappaB and JNK in a PGE2 independent manner in human articular chondrocytes. *Rheumatol Int.* 2008;28:727–736.
45. Urban JP, Smith S, Fairbank JC. Nutrition of the intervertebral disc. *Spine.* 2004;29:2700–2709.
46. Valdes AM, Hassett G, Hart DJ, Spector TD. Radiographic progression of lumbar spine disc degeneration is influenced by variation at inflammatory genes: a candidate SNP association study in the Chingford cohort. *Spine.* 2005;30:2445–2451.
47. Wang YJ, Shi Q, Lu WW, Cheung KC, Darowish M, Li TF, Dong YF, Zhou CJ, Zhou Q, Hu ZJ, Liu M, Bian Q, Li CG, Luk KD, Leong JC. Cervical intervertebral disc degeneration induced by unbalanced dynamic and static forces: a novel in vivo rat model. *Spine.* 2006;31:1532–1538.
48. Yoon EK, Lee WK, Lee JH, Yu SM, Hwang SG, Kim SJ. ERK-1/-2 and p38 kinase oppositely regulate 15-deoxy-delta(12,14)-prostaglandinJ(2)-induced PPAR-gamma activation that mediates dedifferentiation but not cyclooxygenase-2 expression in articular chondrocytes. *J Korean Med Sci.* 2007;22: 1015–1021.
49. Zhang JY, Ma K, Li Y, Zhang YT, Wu LM, Li XR, Pan L, Li LD. Study on therapeutic effects of series of muscone on myocardial infarction canines. *Zhongguo Zhong Yao Za Zhi.* 2006;31: 1702–1705.